ELSEVIER

International Journal of Mass Spectrometry 220 (2002) 313–330

International Journal of Mass Spectrometry

www.elsevier.com/locate/ijms

High resolution study of cluster anion formation in low-energy electron collisions with molecular clusters of CO_2, CS_2, and O_2

S. Barsotti, E. Leber, M.-W. Ruf, H. Hotop*

Fachbereich Physik, Universität Kaiserslautern, D-67663 Kaiserslautern, Germany

Received 19 December 2001; accepted 20 March 2002

Abstract

Using a high resolution (ΔE = 1–2 meV) laser photoelectron attachment (LPA) method, we have studied the formation of $(CO_2)_q^-$ (q = 4–32), $(CS_2)_q^-$ (q = 1, 2, 3, 5), and $(O_2)_q^-$ (q = 5–14) cluster anions in collisions of low-energy electrons (0–200 meV) with molecular clusters of CO_2, CS_2, and O_2 molecules in a skimmed supersonic beam. For CO_2 clusters, the attachment spectrum is dominated by rather narrow vibrational Feshbach resonances (VFRs) of the type $[(CO_2)_{N-1}CO_2(\nu_i)]^-$ which involve a vibrationally excited molecular constituent ($\nu_i \geq 1$ denotes excited vibrational mode). The size-dependent values of the observed redshifts of the VFRs (about 12 meV per added CO_2 unit for small q) in conjunction with their narrow widths and with simple model calculations of the electron binding energies suggest that the size q of the observed $(CO_2)_q^-$ anions is essentially the same ($q = N$ or $N - 1$) as the size N of the neutral precursor $(CO_2)_N$ which captures the electron. For cluster sizes q above 24, a doubling of the VFR peak structure is observed which we tentatively attribute to the transition from icosahedral (low N) to bulk cubic (high N) cluster structure, previously predicted to occur for N around 30. The size distribution in the $(CO_2)_q^-$ anion mass spectrum, due to attachment of electrons with well-defined energies, shows undulatory structure which reflects the presence or absence of VFRs at that particular energy. In contrast, the energy-integrated cluster anion mass spectrum shows a rather smooth dependence on cluster size q. The yield spectra for $(CS_2)_q^-$ cluster anions exhibit an s-wave attachment peak near 0 eV and a smoothly falling cross section towards higher energies without significant structure. In the yield for $(O_2)_q^-$ anions we observe a rise towards 0 eV, indicative of s-wave electron capture, and a slowly varying and essentially structureless attachment continuum between 10 and 200 meV. The attachment characteristics of the different clusters systems are discussed in the light of the basic properties of the monomers. (Int J Mass Spectrom 220 (2002) 313–330)

PACS: 34.80.Ht; 36.40.Wa; 34.80.Gs; 36.40.Qv

Keywords: Cluster anion; Electron attachment; Vibrational Feshbach resonances

1. Introduction

Temporary negative ion states XY^{*-} are known to be crucial for vibrational excitation and negative ion formation in low-energy collisions of electrons with molecules XY and clusters $(XY)_N$ ($N \geq 2$) (described by a set of quantum numbers $\{\alpha\}$ denoting the electronic and ro-vibrational state) [1–6]:

$$(XY)_N\{\alpha\} + e^-(E) \rightarrow (XY)_N{}^{*-} \rightarrow (XY)_N\{\alpha'\} + e^-(E') \quad (1a)$$

* Corresponding author. E-mail: hotop@physik.uni-kl.de

1387-3806/02/$ – see front matter
PII S1387-3806(02)00688-7

$$\rightarrow (XY)_{q-1}Y^- + X + (N-q)XY \quad (q \leq N) \tag{1b}$$

$$\rightarrow (XY)_q{}^- + (N-q)XY \quad (q \leq N) \tag{1c}$$

$$\rightarrow (XY)_N{}^{\ddagger -} \quad (\tau > 100\,\mu s) \tag{1d}$$

Here path (1a) describes elastic ($\alpha = \alpha'$) or inelastic scattering. Process (1b) represents dissociative electron attachment (DEA) while in the reaction (1c) (only relevant for clusters) anion formation proceeds through evaporation of XY constituents. Even if no other stabilising process occurs, the temporary negative ion $(XY)_N{}^{*-}$ ($N \geq 1$) can become metastable with respect to spontaneous re-emission (autodetachment) of the electron, if the electronic energy is rapidly redistributed into internal degrees of freedom (intra- and intermolecular vibration, rotation), thereby yielding the long-lived negative ion $(XY)_N{}^{\ddagger -}$ (1d) (such as $SF_6{}^{\ddagger -}$ from SF_6 [7] or small $(H_2O)_N{}^{\ddagger -}$ anions ($N = 2, 6, 7$) [8]).

Both shape resonances (electrons trapped within a centrifugal barrier) and electronic Feshbach resonances (electrons bound to electronically excited states) are well-known representatives of such temporary negative ion states in which the electron is captured for a time interval long compared to the collision time. For molecular clusters $(XY)_N$ additional features are observed which reflect the effects of the cluster environment on the resonance energy and symmetry [4–6]. One fascinating result in such studies of cluster anion formation is the observation of a prominent resonance at zero energy (indicative of an s-wave attachment process) in cases where such a feature is absent in the monomer [5,9]. The first observations of these 'zero energy resonances' [5,9] for clusters of oxygen [10], carbon dioxide [11–14] and water [15] were made by groups at Innsbruck and Konstanz at broad energy widths of 0.5–1.0 eV, thus preventing the elucidation of possible structure (e.g., due to vibrational effects) and a thorough understanding of the origin of these zero energy peaks. Later, Illenberger and coworkers studied $(O_2)_q{}^-$ ($q = 1$–4) anion formation from oxygen clusters with an energy-selected electron beam of about 0.2 eV width [16–18]; they detected the maximum respective anion yield at energies clearly above zero energy. In 1996, the Innsbruck group [19] had a closer look at anion formation from oxygen clusters, using an energy-selected, magnetically collimated electron beam with a stated energy width around 0.03 eV. They reported the yield for small cluster anions $(O_2)_q{}^-$ ($q = 1$–3) over the energy range 0–1 eV [19,20]. Apart from a resolution-limited peak near-zero energy they detected peak structure starting at about 80 meV with spacings around 110 meV and superimposed on the general drop of the attachment yield towards higher energies. This structure was ascribed to vibrational levels of the oxygen anion solvated in oxygen molecules [20].

Recently, three especially clear examples of prominent resonances in electron collisions with molecules and clusters at very low energies have been observed in DEA to CH_3I molecules [21] and to N_2O [22,23] as well as CO_2 clusters [24], namely vibrational Feshbach resonances (VFRs [21], earlier addressed as nuclear-excited Feshbach resonances [25,26]). VFRs may appear as a prominent peak structure in DEA cross sections (or as a corresponding dip in elastic or inelastic scattering) *below* the vibrational excitation thresholds of the electronic ground state of the molecule (or cluster) if the long-range electron-target interaction is sufficiently strong [21,25–27]. For N_2O clusters, the yield for anion formation (both for heterogeneous $(N_2O)_{q-1}O^-$ and for homogeneous $(N_2O)_q{}^-$ ions, $q \leq N$) was found to be dominated by very sharp VFRs (with widths down to 2.3 meV) [22,23], the peak positions exhibiting very small redshifts which increase weakly with cluster size (by <1 meV per added N_2O unit [23]). For CO_2 clusters (where only homogeneous anion clusters can be formed at low electron energies), the yield for $(CO_2)_q{}^-$ ions ($q \leq N$) is again dominated by VFRs, but with broader widths and higher redshifts, the latter rising by about 12 meV per added CO_2 unit [24]. Thus, the new results show consistently for both N_2O and CO_2 clusters, that the 'zero energy resonances' in these cases are actually comprised of several well-separated VFRs.

In view of all these interesting findings, we considered it worthwhile to extend our high resolution attachment studies in several ways. For CO_2 clusters, we expanded the electron energy range consistently from 0 to 200 meV, and we now cover a larger cluster anion size range ($q = 4$–32). In addition, we present anion mass spectra for selected electron energies as well as an average anion mass spectrum in which the attachment yield has been integrated over electron energy. For the first time, we present electron attachment spectra for the formation of $(O_2)_q^-$ anions from oxygen clusters, measured with very high resolution (energy width $\leq$2 meV). Similarly, we have studied the formation of $(CS_2)_q^-$ ions ($q = 1, 2, 3, 5$) from clusters of carbon disulfide and thus add to the knowledge previously obtained in RET studies involving these clusters [28]. In contrast to the observations for CO_2 clusters, we find no significant vibrational structure in the yields for either oxygen or carbon disulfide cluster anions ($E = 0$–200 meV). The following paper is organised as follows: in Section 2, we describe the essentials of the laser photoelectron attachment (LPA) experiment. In Section 3, we present the experimental results and discuss them in the light of previous work. In Section 4, we conclude with a brief summary and an outlook.

2. Experimental

Our experiment is based on the LPA method [7,8,29]. As illustrated in Fig. 1, energy-variable, monoenergetic electrons are created by photoionisation of atoms in a collimated beam; they interact with the target molecules (clusters) of interest in the region where the photoionisation process takes place. Negative ions due to electron attachment reactions are detected with a quadrupole mass spectrometer. For diagnostics of the target cluster beam, positive ion mass spectra can be generated by electron impact ionisation with an auxiliary electron gun (current around 1 μA, energy here chosen as 85 eV). In the present work, photoelectrons (current: 20–50 pA) are created by two-step photoionisation of potassium atoms [8,30,31]. Both hyperfine components of ground state $^{39}K(4s, F = 1, 2)$ atoms in a collimated beam

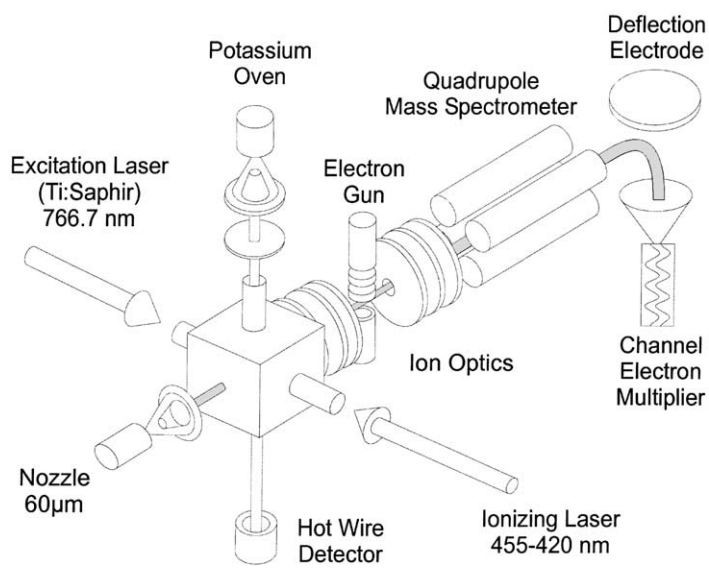

Fig. 1. Experimental setup for mass spectrometric studies of cluster anion formation in collisions of molecular clusters in a collimated supersonic beam with Rydberg electrons or free, monoenergetic photoelectrons, resulting from two-step laser excitation of potassium atoms.

(collimation: 1:400; diameter: 1.5 mm) from a doubly differentially pumped metal vapour oven are transversely excited to the $^{39}K^*(4p_{3/2}, F = 2, 3)$ states by the first sidebands of the electro-optically modulated (frequency: 220.35 MHz) output of a single mode cw Titanium:Sapphire laser ($\lambda_1 = 766.7$ nm). Part of the excited state population is transferred to high Rydberg levels (nd, $(n + 2)$s, $n \geq 12$) or photoionised by interaction with the intracavity field of a broadband (40 GHz) tunable dye laser (power up to 5 W), operated in the blue spectral region ($\lambda_2 = 472$–424 nm, dye Stilbene 3). The energy of the photoelectrons can be continuously varied over the range 0–200 meV by tuning the wavelength of the ionising laser ($\lambda_2 < 455$ nm).

Electrons, created in the overlap volume of the potassium atom beam and the laser beams, may attach to molecules and clusters in a collimated, differentially pumped supersonic beam (diameter in the reaction region 3 mm; diameter of conical nozzle $d_0 = 60$ μm, stagnation pressures p_0 up to 5 bar, nozzle temperatures T_0 between 190 and 300 K), propagating in a direction perpendicular to both the potassium and the laser beams. Anions, generated by electron attachment and drifting out of the essentially field free reaction chamber, are imaged into a quadrupole mass spectrometer ($m/q \leq 2000$ u/e) with a combination of two electrostatic lenses. Since clusters of different size possess nearly the same velocity, but kinetic energies which rise linearly with their size, the ion optics has to be tuned carefully for optimum detection of each cluster ion. The transmitted ions are accelerated to an energy of 1 keV and detected by a differentially pumped off-axis ceramic channel electron multiplier (Sjuts) with very low background ($<0.02\,s^{-1}$).

The reaction volume is surrounded by a cubic chamber made of oxygen free, high conductivity copper, the inner walls of which are coated with colloidal graphite. By applying bias potentials to each face of the cube, dc stray electric fields are reduced to values $F_S \leq 70$ mV/m. Magnetic fields are reduced to values below 2 μT by compensation coils located outside the vacuum apparatus. The electron energy resolution is limited by the bandwidth of the ionising laser ($\Delta E_L \approx 0.15$ meV), residual electric fields ($\Delta E_F \leq 0.3$ meV), the Doppler effect, present in both the photoionisation and in the attachment process (overall Doppler width $\Delta E_D \approx 0.07\sqrt{E}$, ΔE_D and electron energy E in meV), and space charge effects due to K^+ photoions generated in the reaction volume (depending on the K^+ current) [32]. Simulations and measurements indicate that the space charge broadening amounts to about 0.033 meV/pA (FWHM) for the conditions of the attachment experiment [32]. For the sake of normalisation and in situ resolution testing, measurements of SF_6^- formation were frequently carried out, using a seeded supersonic beam of about 0.05% SF_6 in He ($p_0 = 1$ bar, $T_0 = 300$ K). By comparison of the measured anion yield with the known cross section for SF_6^- formation [29] near 0 eV (convoluted with adjustable resolution functions), the effective electron energy spread at low energies can be inferred. From this comparison and the information gained on the energy broadening due to the photoion space charge [32], we estimate the overall energy spread (FWHM) at low energies to be typically 1–2 meV at electron currents in the range 20–50 pA.

3. Results and discussion

In this section we present the experimental results and discuss them in the light of other work. We start with our observations for CO_2 clusters for which cluster anion formation in the energy range 0–200 meV is dominated by series of prominent VFRs (as first reported in [24]) which compose the 'zero energy resonance' [5,9,11–14]. We then describe our results for carbon disulfide clusters and conclude with the observations for oxygen cluster anion formation. At the beginning of each subsection, we briefly review some relevant properties and previous observations for the investigated systems.

3.1. Formation of carbon dioxide cluster anions

Carbon dioxide is linear in its electronic ground state. The lowest vibrationally excited states, labelled

as ($\nu_1\,\nu_2\,\nu_3$), include the bending mode (0 1 0) (82.7 meV), the Fermi-coupled pair of the bending overtone and the symmetric stretch mode (0 2 0)/(1 0 0) (159.4/172.1 meV, average energy 165.7 meV), the Fermi-coupled pair (0 3 0)/(1 1 0) (239.6/257.5 meV; average energy 248.3 meV), the asymmetric stretch mode (0 0 1) (291.3 meV), and the Fermi-coupled triplet (0 4 0)/(1 2 0)/(2 0 0) (317/342/348 meV, average energy 336 meV) [33]. In recent ab initio work, Gutsev et al. [34] calculated basic properties of the ground state molecules and anions of CO_2, OCS, and CS_2. They used both an infinite-order coupled-cluster method with all singles and doubles (CCSD) and non-iterative inclusion of triple excitations (CCSD(T)) as well as Hartree–Fock-density-functional-theory (HFDFT). For carbon dioxide, they found the CO_2^- anion to exist in a bent equilibrium configuration (bond angle 137.8°, electric dipole moment 0.90 D) with a negative adiabatic electron affinity of $EA_{ad}(CO_2) = -0.66$ eV and potential surfaces compatible with the observation of metastable ground state CO_2^- ions [35] (to be distinguished from recently detected, very long-lived CO_2^- anions in high spin states [36,37]). Extensive ab initio (MP2) calculations of the equilibrium structures and stabilities for different isomers of small $(CO_2)_q^-$ cluster anions ($q \leq 6$) have been carried out by Saeki et al. [38,39]. In agreement with photoelectron spectroscopic observations [40], they find that the dimer $C_2O_4^-$ acts as the core in clusters with $q = 2$–5. They predict evaporation energies for dissociation of one CO_2 unit from various isomers of $(CO_2)_q^-$ anions in the range 0.1–0.4 eV, rising substantially (by about 0.15 eV) when going from $q = 5$ to 4. According to molecular dynamics simulations [41–44], neutral carbon dioxide clusters possess icosahedral structure (at least for sizes up to about $N = 20$) with predicted binding energies around 0.14 eV per molecule (for $N = 13$ [44]); at sizes above about $N = 30$, a transition to bulk cubic structure has been predicted, and this bulk structure has been experimentally verified for N above about 100 [43]. Previous experimental work of cluster anion formation in energy-controlled electron collisions with carbon dioxide clusters includes low-resolution beam studies over extended energy ranges [4,11–14], investigations by Rydberg electron transfer (RET) [45–48] and our recent high resolution photoelectron attachment study (energy width about 1 meV) [24]. For details, we refer the reader to these references and other citations therein.

In the present experiments on carbon dioxide clusters, the supersonic beam source was held at room temperature ($T_0 = 300$ K) and at a stagnation pressure of $p_0 = 5$ bar; a 1:1 mixture of carbon dioxide and helium gas was used. In the mass spectrum for positive ion formation due to 85 eV electron impact (Fig. 2a), $(CO_2)_q^+$ ions ($q \geq 1$) dominate the spectrum and exhibit a nearly exponential intensity decrease with rising cluster size q. The fragment ions $(CO_2)_{q-1}O^+$ and $(CO_2)_{q-1}CO^+$ ($q \geq 1$) typically appear with a counting rate which amounts to 5–10% of the neighbouring $(CO_2)_q^+$ ions, respectively. As expected on energetic grounds, only homogeneous ions $(CO_2)_q^-$ ($q > 3$) are observed in the anion mass spectra due to electron attachment to carbon dioxide clusters, both in RET involving $K^{**}(nd)$ atoms ($n = 14$–260) and in free electron attachment ($E = 1$–200 meV). In Fig. 2b and c we show the anion mass spectra due to RET involving $K^{**}(nd)$ Rydberg atoms with $n \approx 20$ (electron binding energy $E_n = 35$ meV) and $n \approx 260$ ($E_n = 0.2$ meV), respectively. Compared with the positive ion spectrum, the RET-induced anion cluster mass spectrum is completely different: the threshold anion spectrum (Fig. 2c) exhibits local maxima at $q = 5$, 10, and a broad maximum around $q = 21$, and local minima at $q = 7$ and 13. Anion cluster mass spectra at lower principal quantum numbers ($n \leq 30$) [24,45–47], such as the one shown in Fig. 2b for $n = 20$, differ significantly from the threshold spectrum in Fig. 2c and indicate a substantial dependence on electron energy over a narrow range, as will be understood through the observations in the free electron attachment spectra. We note that the anion mass spectra (Fig. 2b and c) were measured with the ion optics tuned at cluster size $q = 10$, resulting in signal losses towards larger cluster sizes. A threshold mass spectrum without this drawback (obtained by optimising the ion optics at each cluster anion size) is reproduced in Fig. 8a.

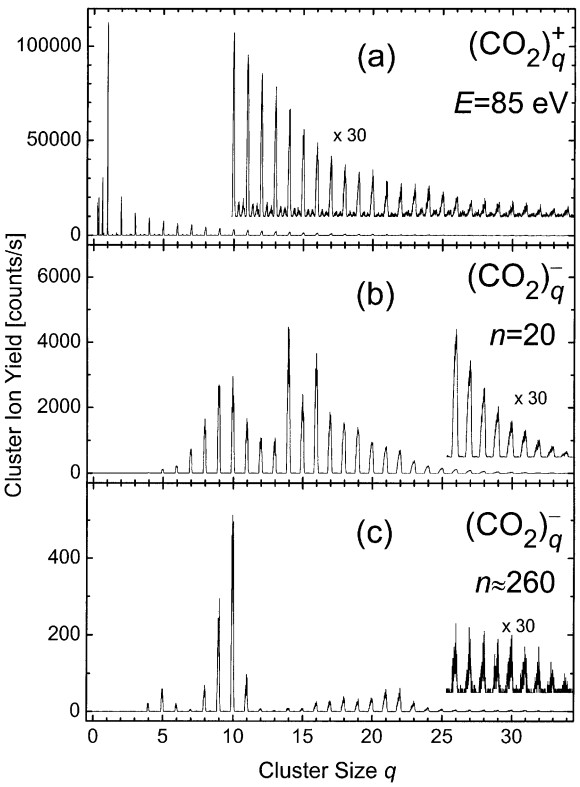

Fig. 2. Mass spectra resulting from electron impact ionisation and electron attachment involving a supersonic beam of molecular clusters of carbon dioxide seeded in helium (50% CO_2, $p_0 = 5$ bar, $T_0 = 300$ K). (a) Spectrum of positive cluster ions due to 85 eV electron impact. The small signals at non-integer cluster sizes correspond to heterogeneous cluster ions $(CO_2)_{q-1}O^+$ and $(CO_2)_{q-1}CO^+$ ($q \geq 1$). (b) Mass spectrum of cluster anions due to Rydberg electron transfer involving $K^{**}(20d)$ atoms ($E_n = 35$ meV). (c) Mass spectrum of cluster anions resulting from threshold electron attachment involving $K^{**}(nd)$ Rydberg atoms with a band of principal quantum numbers around $n \approx 260$ ($E_n \approx 0.2$ meV).

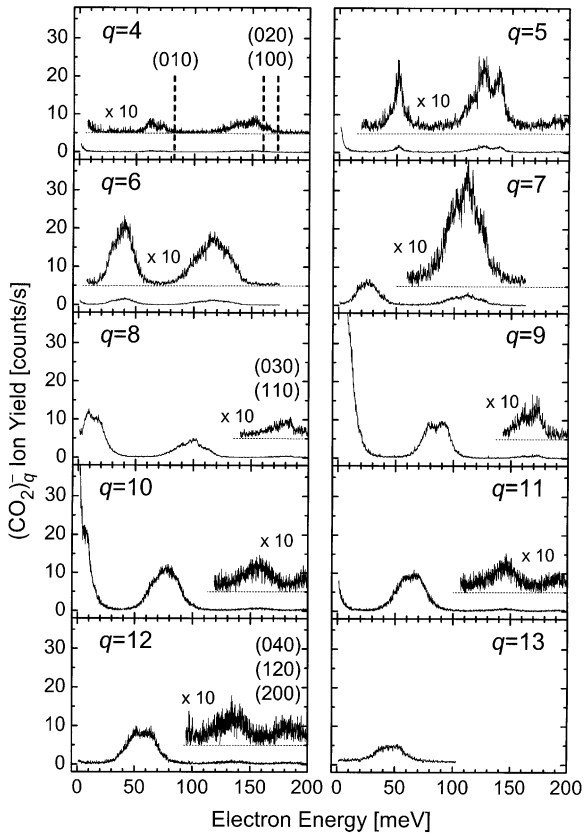

Fig. 3. Yields for the formation of $(CO_2)_q^-$ cluster anions ($q = 4$–13) in free electron attachment to neutral carbon dioxide clusters $(CO_2)_N$ ($q \leq N$). The spectra have a common intensity scale. For $q = 4$, the energy positions of the $(\nu_1\,\nu_2\,\nu_3) = (0\,1\,0)$ and the Fermi-coupled $(0\,2\,0)/(1\,0\,0)$ vibrational modes in the CO_2 monomer are indicated by vertical dashed lines. The incremental redshift of the vibrational Feshbach resonances amounts to about 12 meV per monomer unit.

In Fig. 3 we present the energy-dependent yield for $(CO_2)_q^-$ ($q = 4$–13) cluster anions over the energy range from 1 to 200 meV. For small cluster sizes, two clearly separated series of resonances are observed which exhibit redshifts increasing by about 12 meV per monomer unit. The key spectrum observed for $q = 5$ (in which the peaks exhibit the narrowest widths) shows a distinct zero energy peak (indicative of s-wave attachment), a rather sharp resonance peaking at about 52 meV and a double-peak structure with a centre-of-gravity around 134 meV. We interprete these three peaks to be associated with vibrationally excited temporary cluster anion states (VFRs) of the type $[(CO_2)_{N-1}CO_2(\nu_1\,\nu_2\,\nu_3)]^-$ with $(\nu_1\,\nu_2\,\nu_3) = (0\,1\,0)$ and $(0\,2\,0)/(1\,0\,0)$, respectively, which evolve into the observed long-lived $(CO_2)_5^-$ anions either by redistribution of the vibrational energy among soft modes of the cluster with formation of a metastable cluster ion with $q = N$ or by evaporation of a small number of CO_2 units (most likely N–$q = 1$, see below).

As expected for VFRs, their energies are redshifted from those of the neutral $[(CO_2)_{N-1}CO_2(\nu_1\,\nu_2\,\nu_3)]$ precursor. In contrast to the sharp VFRs observed for N_2O clusters which exhibit small redshifts in the meV range [22,23], the redshift is substantially larger for CO_2 clusters, indicating a stronger interaction of the resonantly captured electron with CO_2 clusters than with N_2O clusters. In line with this observation the resonance widths are larger for CO_2 clusters than for N_2O clusters. For any particular $(CO_2)_q^-$ cluster ion, the width of the observed resonances contains contributions due to the intrinsic resonance widths and resonance positions of all involved neutral precursors which participate in VFR formation, i.e., the observed resonances are in general inhomogeneously broadened. In view of the substantial redshift of about 12 meV per added CO_2 unit and the comparatively narrow intrinsic width of the VFRs, the width in conjunction with the redshift of the VFR allows rather direct conclusions to be drawn on the size *range* of the involved neutral precursors. For $q = 5$ the resonances exhibit the smallest widths, and it is plausible that the attachment spectrum is predominantly associated with a single neutral precursor size (with the possibility of inhomogeneous broadening due to contributions from different conformations for that cluster size). At this narrow peak width, the Fermi-coupled pair (0 2 0)/(1 0 0) is quite well resolved. Interestingly, we find the two peaks at similar intensities in contrast to the situation for vibrationally inelastic scattering of low-energy electrons from CO_2 molecules where, close to the threshold for the pair (0 2 0)/(1 0 0), the higher energy component is excited almost exclusively [49]. This finding has been associated with the influence of a virtual state which has been theoretically predicted for low-energy electron scattering from carbon dioxide [50,51] and recently also been confirmed by total scattering studies at very low energies [52].

For $q = 4$ and ≥ 6, the (0 1 0) resonances appear to be significantly broader than for $q = 5$; this may indicate contributions from two neighbouring neutral precursor sizes, but could also be caused (at least in part) by the influence of different conformations for a particular N. For larger sizes ($q > 7$), additional series

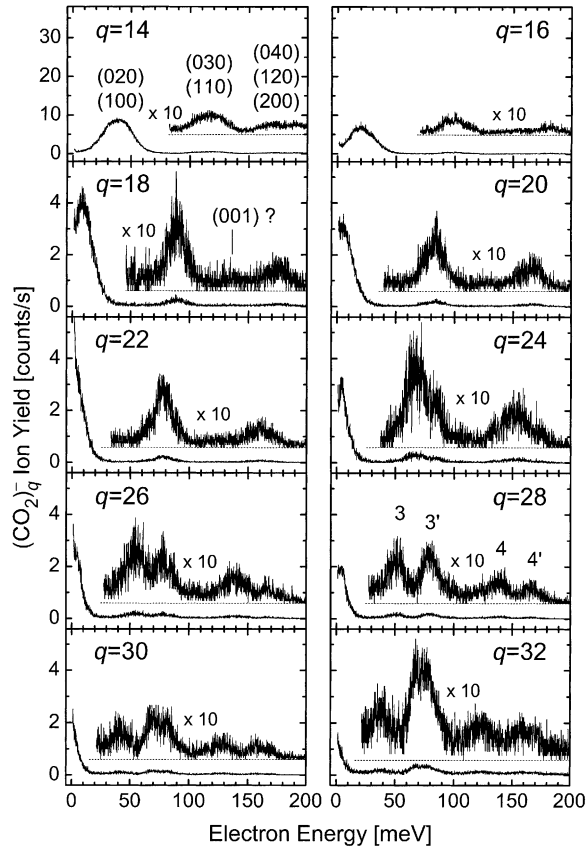

Fig. 4. Yields for the formation of $(CO_2)_q^-$ anions ($q = 14$–32) in free electron attachment to neutral carbon dioxide clusters $(CO_2)_N$, ($q \leq N$). For $q > 24$, a doubling of the Feshbach resonance speak structure is observed which is attributed to the appearance of a second, significantly different attachment state, tentatively identified with bulk cubic structure coexisting with clusters of icosahedral structure.

of peaks, attributed to resonances associated with the Fermi-coupled pair (0 3 0)/(1 1 0) and the triplet (0 4 0)/(1 2 0)/(2 0 0), are successively shifted into the studied energy range. The evolution of these series is clearly seen in Fig. 4 which presents the attachment spectra for $(CO_2)_q^-$ anion formation with sizes $q =$ 14–32. The trends are similar to those observed in Fig. 3, but the redshifts per added molecular unit decrease somewhat at higher q. In some attachment spectra (e.g., for $q = 18$), a weak peak appears to be visible with a redshift compatible with that expected for the (0 0 1) asymmetric stretch vibration. For cluster sizes

q above 24 an interesting doubling of the VFR peak structure is observed in both the (0 3 0)/(1 1 0) ≡ 3 and (0 4 0)/(1 2 0)/(2 0 0) ≡ 4 series; the 3 and 4 series evolve 'normally' towards lower energies with intensities decreasing towards higher q while the 'new' series 3′ and 4′ are observed at 30–40 meV higher energies relative to the 3 and 4 series, respectively, with intensities rising towards larger N. We tentatively attribute these two series to arise from the coexisting icosahedral (series 3, 4) and bulk cubic (series 3′, 4′) cluster structures, with the former losing and the latter gaining importance towards higher N. According to molecular dynamics simulations for carbon dioxide clusters, the icosahedral (low N) to bulk cubic (high N) transition is predicted to occur for sizes around $N = 30$ [43].

In Fig. 5 we summarise the resonance positions E_R of all experimentally observed VFRs. The positions labelled by open symbols correspond to the respective centre-of-gravity for the (0 1 0) series (circles), for the (0 2 0)/(1 0 0) series (squares), for the (0 3 0)/(1 1 0) series (triangles), and for the (0 4 0)/(1 2 0)/(2 0 0) series (stars). For $q > 24$, the latter two series split into the series 3, 4 and 3′, 4′ (see above); the positions of the 3′ and 4′ peaks are shown by full triangles and stars, respectively. For each vibrational series, the resonance position E_R of the VFR mirrors the binding energy E_B ($E_B < 0$, i.e., redshift) of the captured electron in the $[(CO_2)_{N-1}CO_2(\nu_1\,\nu_2\,\nu_3)]^-$ anion state relative to the energy E_N of the neutral $[(CO_2)_{N-1}CO_2(\nu_1\,\nu_2\,\nu_3)]$ cluster which carries the same quanta of intramolecular vibrational energy ($E_R = E_N + E_B$).

In our previous discussion of VFRs in electron attachment to clusters of nitrous oxide [23] and carbon dioxide [24], we presented a simple spherical model for the electron binding energies E_B. The model is based on the assumptions that the geometrical arrangement of the cluster constituents does not play a significant role and that the electron binding energy does not depend on the vibrational state. Correspondingly, the electron cluster interaction energy $V(r)$ simply consists of an appropriately chosen, constant short range interaction U_0 at distances smaller than the cluster radius $R_N = R_0(1.5N)^{1/3}$ (R_0 = effective

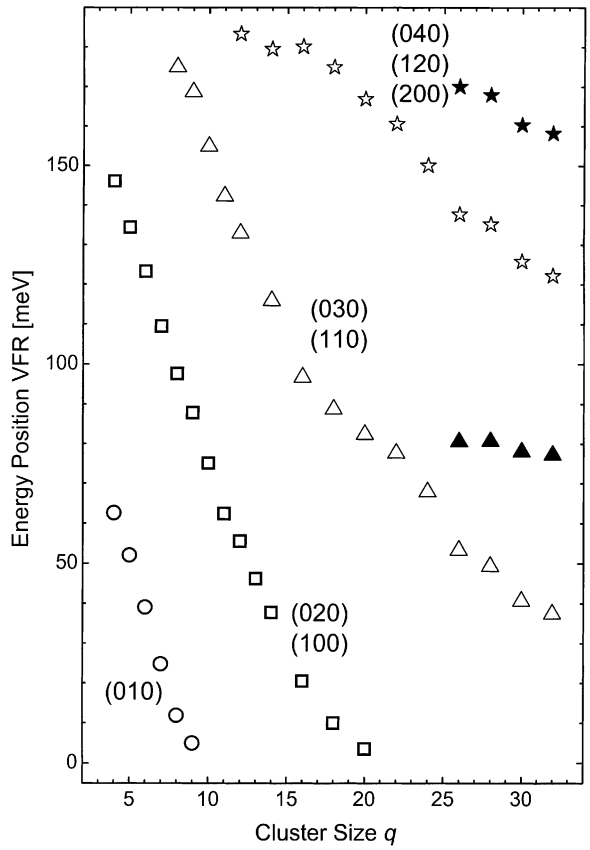

Fig. 5. Centre-of-gravity energy positions of experimentally observed vibrational Feshbach resonances in $(CO_2)_q^-$ cluster anion formation (q = 4–32). (○): ($\nu_1\,\nu_2\,\nu_3$) = (0 1 0) series; (□): average of the (0 2 0)/(1 0 0) series; (△): average of the (0 3 0)/(1 1 0) ≡ 3 series; (☆): average of the (0 4 0)/(1 2 0)/(2 0 0) ≡ 4 series; (▲, ★): new series 3′ and 4′ (see caption for Fig. 4 and text).

radius of a monomer) and of the polarisation attraction $V_{pol} = -Ne^2\alpha(CO_2)/2r^4$ at $R \geq R_N$ (effects associated with weak dipole moments (N_2O) or quadrupole moments of the molecular constituents are neglected in the average over the cluster). As an example, the model potential $V(r)$ with $U_0 = -0.5$ eV, $\alpha(CO_2) = 20a_0^3$ (isotropic monomer polarisability) [53] and $R_0 = 3$ a.u. is illustrated in Fig. 6 for CO_2 clusters with size $N = 10$. We also show the radial wave function $F(r)$ (obtained by numerical integration of the radial Schrödinger equation) and the respective radial probability distribution $r^2F(r)^2$ of the resulting

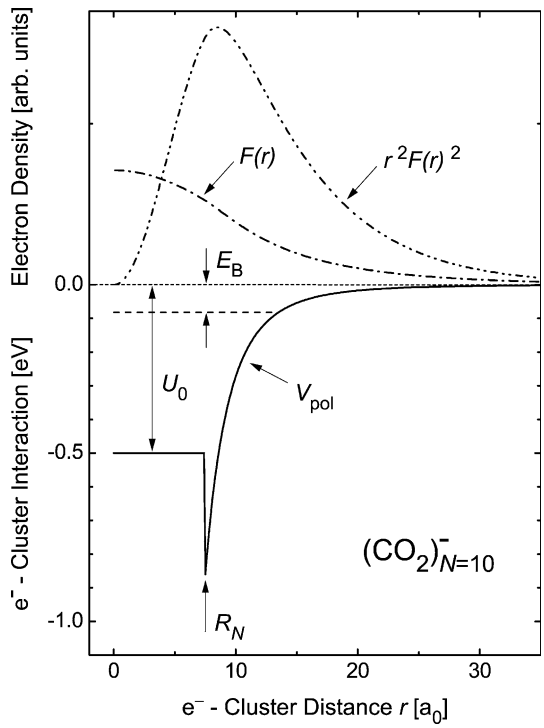

Fig. 6. Radial wave function $F(r)$ (–·–·–) and radial probability distribution $r^2F(r)^2$ (–··–··–) of an electron, weakly bound by $E_B = -0.082$ eV to a $(CO_2)_N$ cluster with $N = 10$, and the model potential $V(r)$ ($U_0 = -0.5$ eV), used to calculate this wave function.

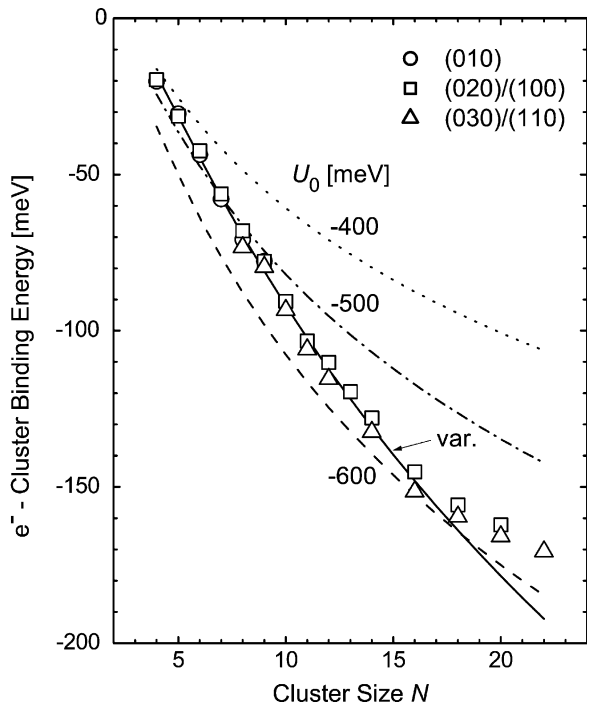

Fig. 7. Comparison between the electron binding energies to $(CO_2)_N$ clusters ($N = 4$–24), as calculated for two different short range interactions U_0, with experimental binding energies, deduced from the centre-of-gravity energy positions of the vibrational Feshbach resonances (assuming $q = N$ and neglecting any influence of the vibrational excitation on the electron binding energy); (○): $(\nu_1\,\nu_2\,\nu_3) = (0\,1\,0)$ series, (□): average of the (0 2 0)/(1 0 0) series, (△): average of the (0 3 0)/(1 1 0) series. The binding energies for the (0 4 0)/(1 2 0)/(2 2 0) series deviate significantly from the behaviour shown consistently by the other three series.

diffuse electron, weakly bound by 0.082 eV in this potential. The shape of the wave function and of the radial probability distribution at shorter range are found to vary rather little with N, while the tail of the wave function towards longer distances attains a larger extension for lower N, i.e., for weaker binding.

Fig. 7 shows calculated electron binding energies to clusters with $N = 4$–22 (dashed lines), as obtained with two different realistic choices of the short range potential U_0 (for further results, see [24]). For comparison, the experimentally derived binding energies $E_{B,exp}$ for the (0 1 0), (0 2 0)/(1 0 0), (0 3 0)/(1 1 0) and (0 4 0)/(1 2 0)/(2 0 0) resonance series, as calculated from the centre-of-gravity resonance positions E_R (Fig. 5) through $E_{B,exp} = E_R - E_q$, are included with the same symbols adopted in Fig. 5. In view of the fact that the intramolecular excitation energies E_N in CO_2 clusters deviate from those in the CO_2 monomer E_1 (listed above) by no more than about ±1 meV (see [24]) we approximate E_N by E_1 for all sizes N of interest. With the assumption $q = N$, used in Fig. 7, reasonable agreement between the calculated and the observed average resonance positions is observed for the choice $U_0 = -0.5$ eV at low N and for $U_0 = -0.6$ eV at higher N. With the weakly N-dependent choice $U_0(N) = aN^{1/3} + b (a = +0.7$ eV, $b = -0.866$ eV) [24], the full curve (labelled var.) is obtained, showing good agreement with the experimentally found binding energies over a broad range of N. In spite of this agreement, the presence

of some evaporation (i.e. $q < N$) cannot be ruled out. If on average one CO_2 molecule were evaporated upon formation of the observed anions ($q = N$–1), the experimental data points in Fig. 7 would have to be shifted to the right by one unit. Calculations with the two parameter potential $U_0(N)$, keeping the term b and raising the factor a by 0.1 eV, yield binding energies which are in satisfactory agreement with the experimental data, assuming $q = N$–1. The combined information contained in the q-dependent redshifts, in the respective resonance widths, in the calculated absolute values of the electron binding energies, and in the slope of the calculated $E_B(N)$ and of the experimental $E_R(q)$ curves allows the conclusion that the main contributions to cluster anion formation are due to $q = N$ and/or $q = N$–1. We are of course aware of the simplicity of the model. For a detailed understanding of these fascinating vibrational resonances large-scale ab initio calculations are needed, such as those recently started [54].

The attachment spectra shown in Figs. 3 and 4 offer the following explanation for the strongly q-dependent ion intensities in the mass spectrum resulting from threshold electron attachment (Fig. 2c) with minima at $q = 7$ and 13, a clear maximum at $q = 10$ and another broad maximum for q around 21. Enhanced cluster ion intensities are found for q-values for which a substantial overlap of a VFR with zero electron energy exists. For $q = 9$, 10, the (0 1 0) resonance has moved close to zero energy, for $q = 16$–22, the (0 2 0)/(1 0 0) resonance pair has a more or less substantial overlap with zero energy. The intensity rise in the threshold attachment mass spectrum (Fig. 2c) from $q = 6$ to 5 may be attributed to an influence of $(CO_2)_N^-$ capture states without intramolecular excitation (but possibly some intermolecular excitation). One would expect such an influence to be even stronger for $(CO_2)_4^-$ formation, but the autodetachment rates of the temporary $(CO_2)_N^{*-}$ negative ions are expected to rise towards low N and thus their survival probability towards stabilisation and detection as long-lived anions should decrease. With the sensitivity of our experiment, $(CO_2)_4^-$ ions were the smallest anions clearly observed in the threshold attachment mass spectrum, see Fig. 2c (in the RET mass spectrum at $n = 20$ (Fig. 2b) $(CO_2)_3^-$ anions are observed in addition, but with very low intensity.) The lower end of the cluster anion mass spectrum at $q = 4$ is also in accord with the calculated increase in CO_2 evaporation energy for $q \leq 4$ [39].

In Fig. 8, we present several selected examples of cluster anion mass spectra, obtained with electrons of different energies. These spectra were obtained with

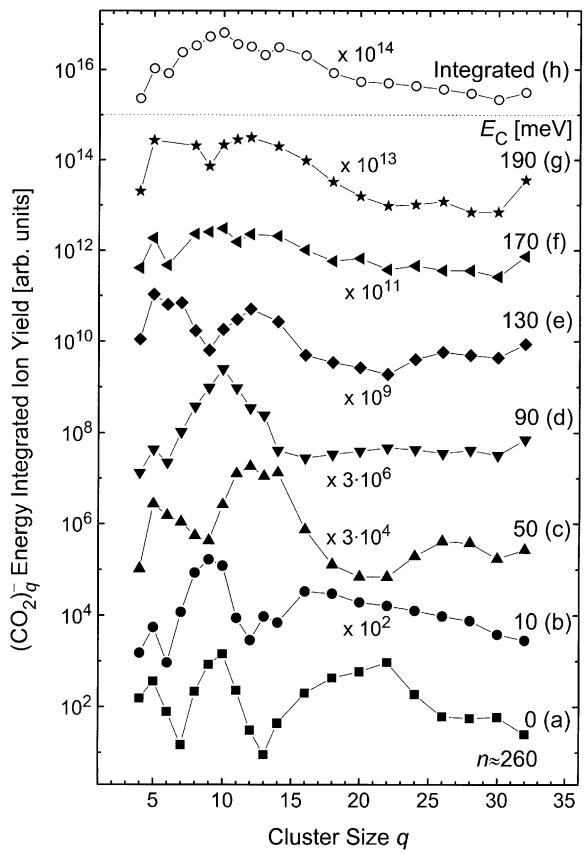

Fig. 8. Mass spectra for $(CO_2)_q^-$ cluster anion formation due to low-energy electron attachment to carbon dioxide clusters. (a)–(g) Anion size dependence as a function of electron energy, as evaluated for selected narrow electron energy bands (±2.5 meV) at the listed average electron energies E_C. Note the shift in the undulatory structure in these mass spectra which is related to the size and energy-dependent appearance of vibrational Feshbach resonances. (h) Energy-averaged anion size dependence, obtained from the respective energy-integrated anion yields. Note the rather smooth size dependence of this mass spectrum as compared to the energy-resolved mass spectra at electron energies below about 0.15 eV.

the ion optics tuned for optimised detection of the respective cluster anion size. Spectrum (a) represents the threshold attachment mass spectrum (RET at $n \approx 260$). The mass spectra (b) to (g) were obtained at the indicated free electron energies by integrating the respective attachment yield functions over an energy interval of 5 meV around the given average electron energy E_C. While spectrum (b) ($E_C = 10$ meV) still retains essential features of the threshold mass spectrum, the other spectra, obtained at higher electron energies, respectively differing by 40 meV, demonstrate varying intensity undulations according to the size-dependent energy locations of the VFRs. When the attachment yield functions are integrated from 1 to 200 meV, the cluster anion mass spectrum labelled 'integrated' is observed in which little structure is left. At larger cluster sizes it shows an overall decrease which is similar to that seen in the positive ion mass spectrum.

3.2. Formation of carbon disulfide cluster anions

Carbon disulfide is linear in its electronic ground state. According to ab initio calculations [34] the adiabatic electron affinity is positive with a value of $EA_{ad} = 0.30$ eV; the stable anion is bent with a bond angle of about 144.5° and an electric dipole moment of +0.46 D. The difference between the theoretical value for EA_{ad} and the experimental result (0.89 eV [55]) appears to be due [34] to very unfavourable Franck–Condon-factors for the transition connecting the respective vibrational ground levels from the anion to the neutral, precluding observation of this transition in the experiment. For optimised linear configurations of CS_2 and CS_2^-, their energies are almost identical with the possibility that the anion is stable against autodetachment by a few meV [34]. This finding is compatible with substantial rate coefficients for the formation of CS_2^- ions in RET experiments [56–58] and can explain observations of long-lived weakly bound CS_2^- ions which undergo electric-field-induced detachment when subjected to fields of only a few kV cm^{-1} [34,56]. Anion formation involving carbon disulfide clusters has been studied by RET [28,59], but to our knowledge no investigations with energy-controlled free electrons have been reported to date. Photodetachment and photodestruction studies of $(CS_2)_q^-$ cluster anions [60–62] in conjunction with ab initio calculations of the anion structures and binding energies [63–65] indicate that a $C_2S_4^-$ core is involved in the $(CS_2)_q^-$ cluster anions with $q \geq 2$ which exhibit the lowest strong photoabsorption band peaking at energies in the range 1.6–1.8 eV.

In the experiments on carbon disulfide clusters, helium gas at a pressure of 4.5 bar (containing 500 ppm SF_6 gas for taking calibration spectra for SF_6^- formation) was bubbled through liquid CS_2, which was held in a stainless steel container with a constant temperature of 289 K (corresponding vapour pressure of CS_2 about 0.34 bar). The resulting He/CS_2 gas mixture was expanded through the 0.06 mm nozzle at a temperature of 300 K. Attachment spectra for $(CS_2)_q^-$ anions with $q = 1$, 2, 3, and 5 were recorded at an electron current of 23 pA. Typical threshold cluster anion intensities I_q, as recorded by RET close to threshold ($n \approx 260$) and normalised to the monomer anion CS_2^- ($I_1 = 1$), amounted to 0.66, 0.50, 0.024 for $q = 2$, 3, 5. Anion mass spectra taken at $n = 20$ showed a relative increase of the monomer anion intensity which we attribute to CS_2^- formation from CS_2 monomers as a result of post-attachment stabilisation (which does not occur at $n \approx 260$).

Fig. 9 presents the yield functions for formation of small carbon disulfide cluster anions with sizes 1, 2, 3, 5 in electron attachment collisions over the energy range 1–150 meV. For all cluster anion sizes, the attachment yield shows a monotonous decline towards higher electron energies. Within the statistical uncertainties no structure is observed. The anion cluster size distribution in the free electron attachment spectra, viewed at any particular electron energy, is close to that observed in the threshold attachment RET mass spectrum.

In comparison to the VFR dominated attachment spectra for carbon dioxide cluster anion formation, the question arises why no vibrational structure is observed for carbon disulfide. One essential difference

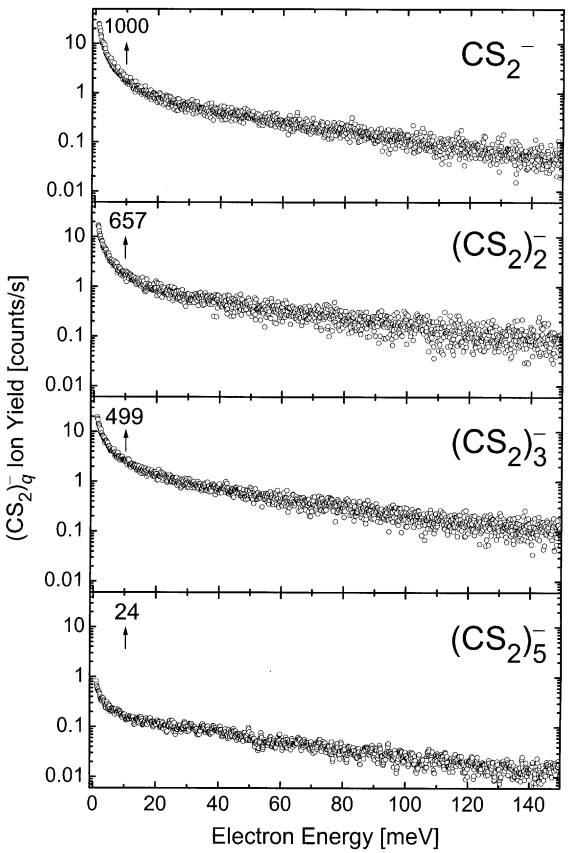

Fig. 9. Yields for the formation of $(CS_2)_q^-$ cluster anions ($q = 1$, 2, 3, 5) in free electron attachment to neutral carbon disulfide clusters $(CS_2)_N$ ($N \geq 2$). The spectra have a common intensity scale. The numbers above the arrows near-zero energy indicate the respective relative anion signals for RET at $n \approx 260$.

between the two systems is the difference in the molecular electron affinities. Carbon dioxide does not form a stable negative ion while CS_2 does (see above). Moreover, temporary CS_2^- ions are efficiently formed in collisions of carbon disulfide molecules with low-energy electrons, as demonstrated in several RET experiments [56–58]. At sufficiently low principal quantum numbers ($n < 25$) energy exchanges occur between the temporary anion and the Rydberg core; correspondingly, anions may be formed with long lifetimes which allow their detection in mass spectrometers. Towards higher n, electrons are still transferred with high efficiency to the carbon disulfide molecule (as demonstrated by the detection of the positive Rydberg core ion [57]), but stabilising energy exchanges become less and less probable with increasing n, such that the temporary anions undergo autodetachment. For carbon dioxide molecules, on the contrary, anions are *not* formed in collisions with free near-zero energy electrons because of the endothermicity of the process. For carbon dioxide clusters, electron attachment is an exothermic process at zero electron energy for any cluster size, $N \geq 2$, but our results clearly show that zero energy electron attachment is very inefficient in producing long-lived cluster anions with sizes below $q = 4$. For $q = 4$, anion formation proceeds through both VFRs and zero energy attachment. The latter process may also occur for smaller clusters ($q = 2$, 3), but the non-observation of long-lived cluster anions with sizes below $q = 4$ indicates that the lifetime of temporary carbon dioxide cluster anions with such a small size is too short to allow efficient detection with our mass spectrometer.

For carbon disulfide clusters, electron attachment at near-zero energies is efficient for any size (including the monomer); the formed temporary cluster anion may evaporate monomers at an energy expense of about 0.17 eV per molecule [28]. In this way reaction (1c) can proceed with an evaporation of one or more monomers (depending on the values of the respective electron affinities and evaporation energies). In collisions with free electrons or Rydberg electrons with sufficiently high principal quantum number long-lived monomer CS_2^- anions are not formed from the neutral monomer. The yield for CS_2^- formation (Fig. 9) thus originates from neutral clusters with sizes $N \geq 2$.

3.3. Formation of oxygen cluster anions

Addition of a π_g electron to the oxygen molecule (equilibrium distance $R_e[O_2(X)] = 120.75$ pm [66]) yields a stable negative ion with an adiabatic binding energy of 0.451(7) eV [67] and an elongated equilibrium distance of $R_e(O_2^-) = 134.7(5)$ pm [67]. The four lowest vibrational levels of the $O_2^-(^2\Pi_g, v')$ anion are truly bound with a vibrational quantum of $\Delta G_{01} = 134.4(8)$ meV [68]. The centre-of-gravity of

the $\nu' = 4$ anion state is located 0.09 eV above the ground state of O_2(X) [69], and the states with $\nu' \geq 4$ are thus subject to autodetachment with decay widths $\Gamma_{\nu'}(E)$ rising strongly ($\propto E^{5/2}$) with electron energy E, as characteristic for a dπ_g-wave shape resonance for the electron–O_2 system; for $\nu' = 6$, the width is about 1 meV [70–72]. Correspondingly, the formation of long-lived oxygen anions in electron collisions at sub electron-volt energies requires rapid collisional stabilisation of the temporary O_2^- anion, as possible in high pressure media [73–75] or for oxygen bound in aggregates (homogeneous or heterogeneous clusters) [5,10,16–18,75,76]. The built-in stabilisation capability of clusters was, e.g., demonstrated in a recent RET study involving oxygen monomers and dimers [77]: while O_2^- formation from O_2 molecules is very inefficient (and only possible through efficient post-attachment interactions with the Rydberg ion core) [57,78] the rate coefficient for O_2^- formation from oxygen dimers was found to exceed that involving monomers by 4 orders of magnitude [77]. Free electron attachment to oxygen clusters was pioneered by the Innsbruck group [10] with a magnetically guided electron beam of about 0.5 eV width. In the energy-dependent yield for $(O_2)_q^-$ anions ($q = 1$, 2, 10) at low energies they found a prominent peak near 0 eV; for large q, the width of this peak was substantially narrower than for $q = 1$ and 2. Some years later, Illenberger and coworkers studied $(O_2)_q^-$ ($q =$ 1–4) anion formation from oxygen clusters with an energy-selected electron beam of about 0.2 eV width [16–18]. At low electron energies, they observed a single, rather broad peak (width between 0.95 eV for $q = 1$ and about 0.8 eV for $q = 4$), located at 0.7 eV for $q = 1$ and at about 0.4 eV for $q \geq 2$ [17]. More recently, the Innsbruck group [19,20] had a closer look at anion formation from oxygen clusters, using an energy-selected, magnetically collimated electron beam with a stated energy width around 0.03 eV. They reported the yield for small cluster anions $(O_2)_q^-$ ($q = 1$–3) over the energy range 0–1 eV. Apart from a resolution-limited peak near-zero energy they detected peak structure starting at about 80 meV with spacings around 110 meV and superimposed on the general drop of the attachment yield towards higher energies. This structure was ascribed to vibrational levels of the oxygen anion solvated in oxygen molecules. With regard to the peak location in the attachment yield functions, these new results are at variance with those of the Berlin group [16–18]. Matejcik et al. [20] suggested that this difference could be due to a distinctly smaller average cluster size in the Berlin experiments (see also the discussion below).

In the present experiments on oxygen clusters, the supersonic beam source was held at temperatures near $T_0 = 190$ K and at a stagnation pressure of $p_0 = 5$ bar; pure O_2 gas was used. Neutral cluster formation was monitored by recording the mass spectrum of positive cluster ions, as produced by electron impact at an electron energy of 85 eV. As documented in Fig. 10a, $(O_2)_q^+$ ions ($q \geq 1$) dominate the spectrum and exhibit a nearly exponential intensity decrease with rising cluster size q. The $(O_2)_{q-1}O^+$ ($q \geq 1$) fragment ions typically appear with a counting rate which amounts to 10–20% of the neighbouring $(O_2)_q^+$ ions, respectively (except for the O_3^+ ion which exhibits an anomalously low intensity in agreement with previous work, see, e.g., [79]).

As expected on energetic grounds, only homogeneous ions $(O_2)_q^-$ ($q \geq 1$) are observed in the anion mass spectra due to electron attachment to oxygen clusters, both in RET involving K**(nd) atoms with principal quantum numbers $n =$ 14–260 (electron binding energies 71–0.2 meV) and in free electron attachment over the energy range $E =$ 1–200 meV. In Fig. 10b and c, we show the anion mass spectra due to RET involving K**(nd) Rydberg atoms with $n = 20$ and ≈260. Compared with the positive ion spectrum, the anion cluster mass spectra are completely different for sizes $q < 10$: they exhibit a maximum at $q = 7$, a drop to a local minimum at $q = 3$ and very little intensity for the monomer anion O_2^-. The spectrum obtained at threshold (i.e., with a band of principal quantum numbers around $n = 260$) has a similar shape as that measured at $n = 20$. More specifically, it was found that the q-dependent cluster anion intensity ratios $I_q(n)/I_{q=7}(n)$ ($q =$ 4–16) were—to within a factor of two or less—independent of principal

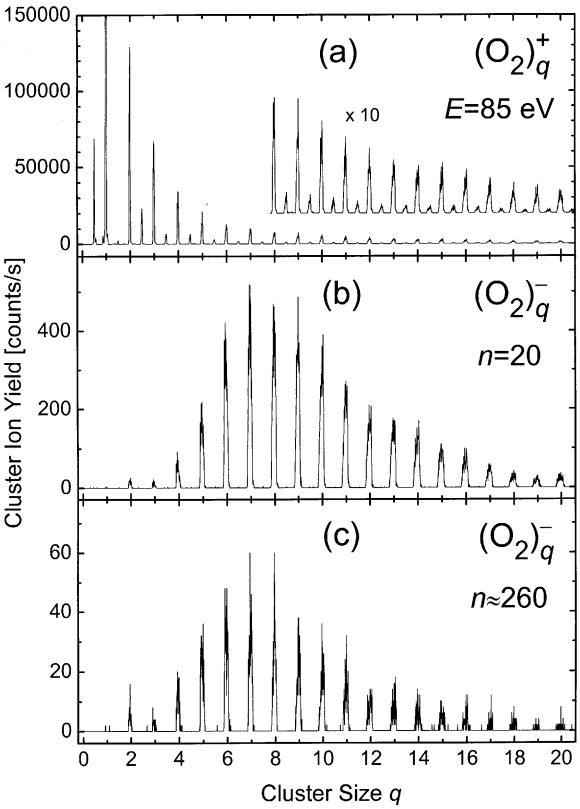

Fig. 10. Mass spectra resulting from electron impact ionisation and electron attachment involving a collimated beam of molecular oxygen clusters (pure oxygen at $p_0 = 5$ bar, $T_0 = 190$ K). (a) Spectrum of positive cluster ions due to 85 eV electron impact. The small signals at non-integer cluster sizes correspond to fragment cluster ions $(O_2)_{q-1}O^+$ ($q \geq 1$). (b) Spectrum of negative cluster ions due to Rydberg electron transfer from $K^{**}(20d)$ atoms. (c) Spectrum of negative cluster ions due to threshold electron attachment involving $K^{**}(nd)$ Rydberg atoms with a band of principal quantum numbers around $n \approx 260$ ($E_n \approx 0.2$ meV).

quantum number ($n = 14$–260). Compared with the present results, the previous RET work [46] over the range $n = 16$–30 (nozzle diameter 60 μm, pure O_2 gas, $T_0 = 200$ K, $p_0 = 5.5$ bar), yielded anion intensities much more concentrated at small sizes q with a peak at $q = 2$ and another maximum at $q = 4$, interpreted to reflect anion cluster stabilities. We attribute this difference primarily to the use of different nozzle shapes: in the previous work the supersonic beam was formed with a sonic nozzle (plane outer surface) while here we use a conical nozzle (see Section 2) which favours cluster formation. It is somewhat surprising, though, to see the weak anion intensities at low q, especially for $q = 1$. In this connection, we note another substantial difference between the present and the earlier [46] work: the time between anion formation and detection at the electron multiplier. While the time intervals, spent from the injection into the quadrupole mass spectrometer to detection are nearly the same in both cases, the time between formation and injection is substantially longer in the present case. Work on $(O_2)_q^-$ anion formation ($q = 1$–70) with a broad distribution of near 0 eV electrons by Walder et al. [80], as studied with a double focussing sector field mass spectrometer, demonstrated strongly different anion mass spectra for the two ion acceleration voltages of 3 and 1.5 keV, respectively. At the higher voltage (Fig. 10a in [80]), the anion mass spectrum peaked at $q = 1$ with a monotonous decrease towards higher q, as seen in previous work from that group [10]. At the lower voltage and thus for enhanced residence times of the anions in the mass spectrometer prior to detection, the anion spectrum peaked at a cluster size around $q = 38$, with little intensity left at low anion cluster sizes (Fig. 10b in [80]). This depletion at smaller cluster sizes was tentatively attributed to autodetachment processes with size-dependent lifetimes [80] (shorter lifetime for smaller cluster anion size).

In Fig. 11, we show free electron attachment spectra for the formation of size-selected $(O_2)_q^-$ anions ($q = 5$–14), taken at an electron current of 50 pA over the energy range 1–200 meV. In view of the low counting rates and the absence of sharp structure in the spectra, we have summed data points for 2 meV intervals in the range 1–11 meV and for 5 meV intervals in the range 10–200 meV. Following a steep drop above 0 eV, the anion yield is almost constant over much of the studied energy range. Compared to other systems (such as CO_2, N_2O or CS_2 cluster anion formation), our results for oxygen clusters show a relatively weak anion yield at low energies. In order to quantify this statement, we have compared the positive and negative cluster ion intensities for O_2 and CO_2 clusters for

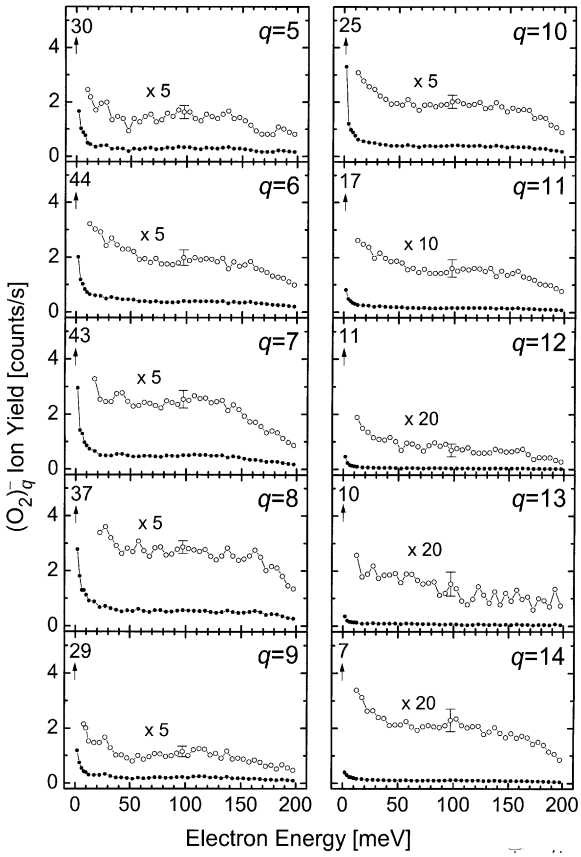

Fig. 11. Yields for the formation of $(O_2)_q^-$ cluster anions ($q = 5$–14) due to free electron attachment to neutral oxygen clusters $(O_2)_N$ ($N > q$). The spectra have a common intensity scale. The numbers above the arrows near-zero energy give the cluster anion signal (counts/s) for RET at $n \approx 260$.

sizes around $q = 8$; we regard the ratio $R = I_-/I_+$ of the intensities for negative to positive cluster ions as a coarse estimate for the relative efficiency of anion formation (considering positive ion formation at $E =$ 85 eV to occur with similar efficiency for both O_2 and CO_2 clusters). To obtain representative anion signals I_- which are free of the localised influence associated with resonances in the attachment yield, we use energy-averaged anion counting rates (obtained by integration over the electron energy range 1–200 meV). The ratios R for CO_2 cluster ion formation exceed those for O_2 cluster formation by about a factor of 10.

In contrast to the findings of the Innsbruck group for $(O_2)_q^-$ formation ($q = 1$–3) [19,20], no clear peak structure is observed in the present attachment spectra ($q = 5$–14). In view of the much improved resolution of the LPA experiment, we should have been able to detect at least the peak structure, located near 80 meV in the Innsbruck data, if such structure did in fact exist in the cluster anion yield for sizes $q =$ 5–14. It is thus of interest to present the scenario, by which—according to the arguments and model calculations presented in [20]—$(O_2)_q^-$ anions ($q = 1$–3) are formed. Matejcik et al. [20] viewed the attachment process to proceed in such a way that the incoming electron is primarily trapped at one oxygen molecule in neutral clusters with sizes dominated by the range $N = 10$–20. Subsequent substantial evaporation then yields the observed anions according to the following reaction scheme:

$$e^-(E) + (O_2)_N \rightarrow (O_2)_N{}^{*-} \rightarrow (O_2)_q{}^- + (N-q)O_2 \quad (2)$$

For this reaction to be exothermic at zero electron energy, the total binding energy of the $(O_2)_q^-$ ion (composed of the adiabatic electron affinity of O_2 plus the bond energies of the additional $(q-1)$ O_2 molecules) has to exceed the total binding energy E_N of the neutral precursor cluster of size N. In particular, O_2^- formation requires that E_N be smaller than $EA_{ad}(O_2) = 0.451(8)$ eV (adiabatic electron affinity of O_2 [67]). According to calculations in [20], scaled to reproduce the cohesive energy of bulk oxygen, the total binding energy of neutral $(O_2)_N$ clusters becomes larger than $EA_{ad}(O_2)$ for $N \geq 14$. Correspondingly, process (2) for $q = 1$ is energetically not possible when zero energy electrons attach to very cold clusters with $N \geq 14$, but may proceed when the electrons possess a sufficient amount of kinetic energy E (for $N = 20$, the threshold energy for O_2^- formation amounts to about $E = 0.3$ eV). In contrast, formation of $(O_2)_q^-$ anions with $q \geq 2$ is exothermic for all neutral sizes up to about $N = 25$ even at zero electron energy. If a size *range* of neutral clusters is active as precursor in the cluster anion formation of a particular size according to (2), the observation of vibrational structure implies a sufficiently small inhomogeneous

broadening of the vibrational resonance. Model calculations of the distribution function of the adiabatic electron affinity of clusters with sizes $N = 10$, 15 and 20 (Fig. 8 in [20]) for the various cluster structures and positions of the solvated O_2^- in the cluster showed the following behaviour at low cluster temperatures T_C: for sufficiently cold (i.e., solid) clusters ($T_C \leq 20$ K), the width (FWHM) of the distribution for a particular N amounted to about 0.07 eV. Moreover, the peak position of the distribution remained nearly the same (close to 0.8 eV) for $N = 15$ and 20 while it shifted by to 0.7 eV for $N = 10$. For (partially) molten clusters (as shown for $T_C = 40$ K [20]), the distribution was found to become wider by about a factor of 2 and thus too broad to resolve vibrational structure even for a single precursor size. These calculations thus suggest that the absence of vibrational structure in our attachment spectra may be due to the fact that the oxygen clusters in our experiment were not sufficiently cold. From simulations of the peak structure, assuming solid oxygen clusters with a certain size range, Matejcik et al. concluded that neutral clusters around $N = 15$ (ranging from 13 to 20) are responsible for their attachment spectra with $q = 1$–3 (Figs. 4 and 9 in [20]). This size selectivity was not explained. The authors also did not comment why the same range should be responsible for the formation of O_2^-, O_4^-, and O_6^- ions (note that the peak structures for cluster anions with $q = 1$–3 was found to be located—within their uncertainties—at the same energies). For O_2^- formation, one would actually expect (in view of the energetic restriction that N may not be larger than 13) that the average size of the neutral clusters involved in anion formation is significantly smaller than for dimer and trimer anion formation with the result that the peaks in the O_2^- attachment spectrum appear at higher energies than those in the dimer and trimer anion spectra.

In this connection it is appropriate to recall that the Berlin group found a clear difference in the peak location of the yield for $(O_2)_q^-$ formation between $q = 1$ (0.7 eV) and $q \geq 2$ (0.4 eV) [16–18]. This difference is, on the one hand, compatible with a scenario that, on average, O_2^- formation involves neutral clusters of smaller size than those responsible for $(O_2)_q^-$ ($q \geq 2$) formation. In the light of the Innsbruck observations (yielding the maximum yield of small oxygen cluster anions at 0 eV) [19,20] the Berlin results may be possibly understood if—as proposed in [20]—the neutral precursor clusters had a substantially smaller size in the Berlin experiment. It is desirable for a better understanding of these different observations to carry out additional experiments (if possible with energy width $\leq$30 meV) which allow to vary the neutral cluster size distribution and the cluster temperature.

4. Conclusions

Using a high resolution ($\Delta E \approx$ 1–2 meV) LPA method, we have studied the formation of $(CO_2)_q^-$ ($q = 4$–32), $(CS_2)_q^-$ ($q = 1$, 2, 3, 5) and $(O_2)_q^-$ ($q = 5$–14) cluster anions in collisions of low-energy electrons (0–200 meV) with molecular clusters of CO_2, CS_2 and O_2 molecules in a skimmed supersonic beam. For CO_2 clusters, the attachment spectrum is dominated by rather narrow VFRs of the type $[(CO_2)_{N-1}CO_2(\nu_i)]^-$ which involve a vibrationally excited molecular constituent ($\nu_i \geq 1$ denotes excited vibrational mode) and a diffuse electron, weakly bound to the cluster by long range forces (redshift about 12 meV per added CO_2 for small q). For q up to about 24, the size-dependent values of the observed redshifts of the VFRs in conjunction with their narrow widths and with model calculations of the electron binding energies suggest that the size q of the observed $(CO_2)_q^-$ anions is essentially the same ($q = N$ or $N - 1$) as the size N of the neutral precursor $(CO_2)_N$ which captures the electron. For cluster sizes q above 24 a doubling of the VFR peak structure is observed which we tentatively attribute to the transition from icosahedral (low N) to bulk cubic (high N) cluster structure, predicted to occur for N around 30 [43]. The size distribution in the $(CO_2)_q^-$ anion mass spectrum, due to attachment of electrons with well-defined energies, shows undulatory structure which reflects the presence or absence of VFRs at that particular energy. In contrast, the energy-integrated cluster anion mass spectrum shows a smooth dependence on cluster size

q which is similar to that observed in the positive $(CO_2)_q^+$ cluster ion mass spectrum, generated by 85 eV electron impact. The yield spectra for $(CS_2)_q^-$ cluster anions show an s-wave attachment peak near 0 eV and exhibit a smoothly falling cross section towards higher energies with no significant structure.

In the yield for $(O_2)_q^-$ anions (q = 5–14), we observe a rise towards 0 eV, indicative of s-wave electron capture, and a slowly varying and essentially structureless attachment continuum between 10 and 200 meV. Vibrational peak structure, previously reported by the Innsbruck group [19,20] in the yields for small $(O_2)_q^-$ anions (q = 1–3) at energies near 80 and 190 meV and interpreted as solvation-shifted $O_2^-(^2\Pi_g, \nu' = 7, 8)\cdot(O_2)_{N-1}$ resonances ($N \geq 10$) which decay to the detected $(O_2)_q^-$ anions by evaporation of a substantial number of O_2 molecules, appears to be absent in our data for q = 5–14. Possibly, the neutral clusters $(O_2)_N$ were not sufficiently cold (and thus solid) in our experiment such as to yield—as suggested in [20]—a sufficiently small inhomogeneous broadening of the resonances when averaging over those neutral cluster sizes N which are active as precursors in the production of the detected cluster anion size q. Differences between the attachment spectra for oxygen cluster anions, as observed by the Innsbruck [19,20], Berlin [16–18] and our group, indicate the need for additional experiments in order to clarify the situation.

In conclusion, we note that we have recently investigated cluster anion formation involving clusters of carbonyl sulfide OCS in order to see the evolution of the attachment behaviour from CO_2 via OCS to CS_2. Clear vibrational resonance structure has been observed in the yields for small homogeneous $(OCS)_q^-$ and heterogeneous $(OCS)_{q-1}O^-$ cluster anions, as will be reported in a future publication.

Acknowledgements

This work was supported by the Deutsche Forschungsgemeinschaft (Forschergruppe *Niederenergetische Elektronenstreuprozesse*) and through the Zentrum für Lasermesstechnik und Diagnostik. We gratefully acknowledge I.I. Fabrikant, J.M. Weber, P. Marinkovic, A. Gopalan and J. Bömmels for their cooperation and T. Sommerfeld, L.S. Cederbaum, D.J. Wales and U. Buck for helpful discussions.

References

[1] G.J. Schulz, Rev. Mod. Phys. 45 (1973) 423.
[2] L.G. Christophorou (Ed.), Electron–Molecule Interactions and their Applications, Vols. 1 and 2, Academic Press, New York, 1984.
[3] M. Allan, J. Electron Spectrosc. 48 (1989) 219.
[4] R.N. Compton, in: N. Oda, K. Takayanagi (Eds.), Electronic and Atomic Collisions, North-Holland, Amsterdam, 1980, p. 251.
[5] T.D. Märk, Int. J. Mass Spectrom. Ion Process. 107 (1991) 143.
[6] O. Ingólfsson, F. Weik, E. Illenberger, Int. J. Mass Spectrom. Ion Process. 155 (1996) 1.
[7] (a) D. Klar, M.-W. Ruf, H. Hotop, Chem. Phys. Lett. 189 (1992) 448;
(b) D. Klar, M.-W. Ruf, H. Hotop, Aust. J. Phys. 45 (1992) 263.
[8] J.M. Weber, E. Leber, M.-W. Ruf, H. Hotop, Eur. Phys. J. D 7 (1999) 587.
[9] A. Stamatovic, in: H.B. Gilbody, W.R. Newell, F.H. Read, A.C.H. Smith (Eds.), Electronic and Atomic Collisions, Elsevier, Amsterdam, 1988, p. 729.
[10] (a) T.D. Märk, K. Leiter, W. Ritter, A. Stamatovic, Phys. Rev. Lett. 55 (1985) 2559;
(b) T.D. Märk, K. Leiter, W. Ritter, A. Stamatovic, Int. J. Mass Spectrom. Ion Process. 74 (1986) 265.
[11] A. Stamatovic, K. Stephan, T.D. Märk, Int. J. Mass Spectrom. Ion Proc. 63 (1985) 37.
[12] A. Stamatovic, K. Leiter, W. Ritter, K. Stephan, T.D. Märk, J. Chem. Phys. 83 (1985) 2942.
[13] M. Knapp, D. Kreisle, O. Echt, K. Sattler, E. Recknagel, Surf. Science 156 (1985) 313.
[14] M. Knapp, O. Echt, D. Kreisle, T.D. Märk, E. Recknagel, Chem. Phys. Lett. 126 (1986) 225.
[15] (a) M. Knapp, O. Echt, D. Kreisle, E. Recknagel, J. Chem. Phys. 85 (1986) 636;
(b) M. Knapp, O. Echt, D. Kreisle, E. Recknagel, J. Phys. Chem. 91 (1987) 2601.
[16] R. Hashemi, E. Illenberger, Chem. Phys. Lett. 187 (1991) 623.
[17] T. Jaffke, R. Hashemi, L.G. Christophorou, E. Illenberger, Z. Phys. D 25 (1992) 77.
[18] R. Hashemi, T. Jaffke, L.G. Christophorou, E. Illenberger, J. Phys. Chem. 96 (1992) 10605.
[19] S. Matejcik, A. Kiendler, P. Stampfli, A. Stamatovic, T.D. Märk, Phys. Rev. Lett. 77 (1996) 3771.
[20] S. Matejcik, P. Stampfli, A. Stamatovic, P. Scheier, T.D. Märk, J. Chem. Phys. 111 (1999) 3548.

[21] A. Schramm, I.I. Fabrikant, J.M. Weber, E. Leber, M.-W. Ruf, H. Hotop, J. Phys. B 32 (1999) 2153.
[22] J.M. Weber, E. Leber, M.-W. Ruf, H. Hotop, Phys. Rev. Lett. 82 (1999) 516.
[23] E. Leber, S. Barsotti, J. Bömmels, J.M. Weber, I.I. Fabrikant, M.-W. Ruf, H. Hotop, Chem. Phys. Lett. 325 (2000) 345.
[24] E. Leber, S. Barsotti, I.I. Fabrikant, J.M. Weber, M.-W. Ruf, H. Hotop, Eur. Phys. J. D 12 (2000) 125.
[25] W. Domcke, L.S. Cederbaum, J. Phys. B 14 (1981) 149.
[26] J. Gauyacq, A. Herzenberg, Phys. Rev. A 25 (1982) 2959.
[27] A.Ch. Sergenton, L. Jungo, M. Allan, Phys. Rev. A 61 (2000) 062702.
[28] C. Desfrancois, N. Khelifa, J.P. Schermann, T. Kraft, M.-W. Ruf, H. Hotop, Z. Phys. D 27 (1993) 365.
[29] D. Klar, M.-W. Ruf, H. Hotop, Meas. Sci. Technol. 5 (1994) 1248.
[30] J.M. Weber, I.I. Fabrikant, E. Leber, M.-W. Ruf, H. Hotop, Eur. Phys. J. D 11 (2000) 247.
[31] I.D. Petrov, V.L. Sukhorukov, E. Leber, H. Hotop, Eur. Phys. J. D 10 (2000) 53.
[32] J. Bömmels, E. Leber, A. Gopalan, J.M. Weber, S. Barsotti, M.-W. Ruf, H. Hotop, Rev. Sci. Instrum. 72 (2001) 4098.
[33] G. Herzberg, in: Molecular Spectra and Molecular Structure II: Infrared and Raman Spectra of Polyatomic Molecules, Van Nostrand Reinhold, New York, 1945.
[34] G.L. Gutsev, R.J. Bartlett, R.N. Compton, J. Chem. Phys. 108 (1998) 6756.
[35] R.N. Compton, P.W. Reinhardt, C.D. Cooper, J. Chem. Phys. 63 (1975) 3821.
[36] M.K. Raarup, H.H. Andersen, T. Andersen, J. Phys. B 32 (1999) L659.
[37] A. Dreuw, L.S. Cederbaum, J. Phys. B 32 (1999) L665.
[38] M. Saeki, T. Tsukuda, S. Iwata, T. Nagata, J. Chem. Phys. 111 (1999) 6333.
[39] M. Saeki, T. Tsukuda, T. Nagata, Chem. Phys. Lett. 340 (2001) 376.
[40] T. Tsukuda, M.A. Johnson, T. Nagata, Chem. Phys. Lett. 268 (1997) 429.
[41] R.T. Etters, K. Flurchick, R.P. Pan, V. Chandrasekharan, J. Chem. Phys. 75 (1981) 929.
[42] M. Tsukada, N. Shima, S. Tsuneyuki, H. Kageshima, T. Kondow, J. Chem. Phys. 87 (1987) 3927.
[43] G. Torchet, M.-F. Feraudy, A. Boutin, A.H. Fuchs, J. Chem. Phys. 105 (1996) 3671.
[44] J.-B. Maillet, A. Boutin, S. Buttefey, F. Calvo, A.H. Fuchs, J. Chem. Phys. 109 (1998) 329.
[45] T. Kondow, J. Phys. Chem. 91 (1987) 1307.
[46] T. Kraft, M.-W. Ruf, H. Hotop, Z. Phys. D 14 (1989) 179.
[47] F. Misaizu, K. Mitsuke, T. Kondow, K. Kuchitsu, J. Chem. Phys. 94 (1991) 243.
[48] T. Kraft, M.-W. Ruf, H. Hotop, Z. Phys. D 18 (1991) 403.
[49] M. Allan, Phys. Rev. Lett. 87 (2001) 033201.
[50] H. Estrada, W. Domcke, J. Phys. B 18 (1985) 4469.
[51] L.A. Morgan, Phys. Rev. Lett. 80 (1998) 1873.
[52] D. Field, N.C. Jones, S.L. Lunt, J.-P. Ziesel, Phys. Rev. A 64 (2001) 022708.
[53] D.R. Lide (Ed.), CRC Handbook of Chemistry and Physics, 76th Edition, Chemical Rubber Company, Boca Raton, FL, 1995.
[54] T. Sommerfeld, private communication.
[55] J.M. Oakes, G.B. Ellison, Tetrahedron 42 (1986) 6263.
[56] A. Kalamarides, C.W. Walter, K.A. Smith, F.B. Dunning, J. Chem. Phys. 89 (1988) 7226.
[57] K. Harth, M.-W. Ruf, H. Hotop, Z. Phys. D 14 (1989) 149.
[58] H.S. Carman Jr, C.E. Klots, R.N. Compton, J. Chem. Phys. 92 (1993) 5751.
[59] T. Kondow, K. Mitsuke, J. Chem. Phys. 83 (1985) 2612.
[60] K.H. Bowen, J.G. Eaton, in: R. Naaman, Z. Vager (Eds.), The Structure of Small Molecules and Ions, Plenum Press, New York, 1988, p. 147.
[61] T. Tsukuda, T. Hirose, T. Nagata, Chem. Phys. Lett. 279 (1997) 179.
[62] T. Maeyama, T. Oikawa, T. Tsumura, N. Mikami, J. Chem. Phys. 108 (1998) 1368.
[63] K. Hiraoka, S. Fujimaki, G. Aruga, S. Yamabe, J. Phys. Chem. 98 (1994) 1802.
[64] A. Sanov, W.C. Lineberger, K.D. Jordan, J. Phys. Chem. A 102 (1998) 2509.
[65] S.W. Zhang, C.G. Zhang, Y.T. Yu, B.Z. Mao, F.C. He, Chem. Phys. Lett. 304 (1999) 265.
[66] K.P. Huber, G. Herzberg, Molecular Spectra and Molecular Structure IV. Constants of Diatomic Molecules, van Nostrand Reinhold, New York, 1979.
[67] M.J. Travers, D.C. Cowles, G.B. Ellison, Chem. Phys. Lett. 164 (1989) 449.
[68] C.G. Bailey, D.J. Lavrich, D. Serxner, M.A. Johnson, J. Chem. Phys. 105 (1996) 1807.
[69] J.E. Land, W. Raith, Phys. Rev. A 9 (1974) 1592.
[70] D. Field, G. Mrotzek, D.W. Knight, S. Lunt, J.-P. Ziesel, J. Phys. B 21 (1988) 171.
[71] K. Higgins, C.J. Gillan, P.G. Burke, C. Noble, J. Phys. B 28 (1995) 3391.
[72] M. Allan, J. Phys. B 28 (1995) 5163.
[73] F. Bloch, N.E. Bradbury, Phys. Rev. 48 (1935) 689.
[74] L.G. Christophorou, Adv. Electron. Electron Phys. 46 (1978) 55.
[75] Y. Hatano, H. Shimamori, in: L.G. Christophorou (Ed.), Electron and Ion Swarms, Pergamon Press, New York, 1981, p. 103.
[76] Y. Hatano, Aust. J. Phys. 50 (1997) 615.
[77] J. Kreil, M.-W. Ruf, H. Hotop, I. Ettischer, U. Buck, Chem. Phys. 239 (1998) 459.
[78] C.W. Walter, B.G. Zollars, C.B. Johnson, K.A. Smith, F.B. Dunning, Phys. Rev. A 34 (1986) 4431.
[79] A. Binet, J.P. Visticot, J.M. Mestdagh, J. Cuvellier, P. de Pujo, J. Berlande, Int. J. Mass Spectrom. Ion Process. 83 (1988) 13.
[80] G. Walder, D. Margreiter, C. Winkler, A. Stamatovic, Z. Herman, T.D. Märk, J. Chem. Soc., Faraday Trans. 86 (1990) 2395.